Fast Communications

J. Synchrotron Rad. (1999). **6**, 59–61

Production of synchrotron X-ray biprism interference patterns with control of fringe spacing

A. R. Lang* and A. P. W. Makepeace

H. H. Wills Physics Laboratory, University of Bristol, Tyndall Avenue, Bristol BS8 1TL, UK. E-mail: a.r.lang@bristol.ac.uk

(*Received 9 December 1998; accepted 19 January 1999*)

An X-ray biprism has been constructed from a pair of rectangular-section polished diamond bars meeting edge-to-edge, and rotatable about the prism axis so as to vary the convergence of the refracted beams. Interference patterns have been recorded at wavelengths of 0.08, 0.096 and 0.11 nm with good agreement between calculated and observed fringe spacings. Application of the fringe-observing arrangement employed in this work to the assessment of X-ray source characteristics is proposed.

Keywords: coherence; X-ray optics; biprism interference patterns; X-ray source characteristics assessment.

1. Introduction

Ways of usefully exploiting the collimation and spatial coherence of synchrotron X-ray beams are being intensively investigated, *e.g.* Raven *et al.* (1996), Cloetens *et al.* (1996), Cloetens, Pateyron-Salomé *et al.* (1997), Espeso *et al.* (1998). Here we report the successful recording of X-ray Fresnel biprism interference patterns with the help of a novel biprism design, and we indicate how it could be employed in the experimental assessment of X-ray source characteristics. Our experiments were performed at the SRS, Daresbury Laboratory, UK, on station 7.6 terminating the 80 m-long beamline. They demonstrate that the transverse (or lateral) coherence length D_t is great enough in the vertical plane for informative X-ray interference experiments to be performed there. [For wavelength λ, beamline length L and source linear dimension s, D_t is approximately $\lambda L/2s$ (Born & Wolf, 1980)]. The good collimation at station 7.6 deriving from a small source vertical FWHM of 0.23 mm has previously been exploited for high-resolution radiographic imaging of non-absorbing objects, in particular of $\leq$100 µm-diameter faceted CVD diamond crystallites (Lang *et al.*, 1997). Such radiographs are generally recorded with a specimen-to-photoplate distance P of $\sim$0.1 m, when refractive deviation of transmitted beams, as calculated by geometrical optics, adequately accounts for the image structure, as it does also for calculating the major focusing properties of X-ray refracting lenses (Snigirev *et al.*, 1998). By using as test specimen a CVD diamond film in which sloping sides of adjacent crystallites met to form V-groove re-entrants (X-ray analogues of Fresnel biprisms), and by extending specimen-to-photoplate distances to >1 m, well into the Fresnel/Fraunhofer diffraction domains, reasonably promising evidence of biprism-type interference was obtained (Lang & Makepeace, 1999). Now, following construction and use of a larger-scale biprism, well defined interference patterns have been produced showing fringe spacings agreeing well with theory.

2. Experiment and discussion

Fig. 1 shows the biprism design. Two similar well polished rectangular-section single-crystal diamond bars, 5 mm long, are aligned so that an edge of one meets an edge of the other. The edges used were selected by optical microscopy as being free (or almost free) from notch damage. Bars A and B are cemented to a larger rectangular-section diamond block (not shown), 2 mm lengths of A and B being used for bonding to the block, leaving a 3 mm-long biprism protruding for X-ray transmission. The biprism assembly was mounted on a goniometer head attached to a shaft held horizontally in a rotary stage. Laser reflections from the surfaces of A and B facilitated setting the biprism axis horizontal and normal to the X-ray beam. In the expression $n = 1 - \delta$ for the X-ray refractive index n, δ is proportional to λ^2 but is always so small that the angular deviation ε produced by each half of the biprism is simply $(\tan\alpha_1 + \tan\alpha_2)\delta$. This gives $2\varepsilon = 4\delta$ at minimum deviation and $2\varepsilon = 8\delta$ when the biprism assembly rotation ρ is 30°.

Wavelength selection was performed by a flat single-crystal silicon monochromator placed downstream of the biprism, using the near-symmetrical 004 reflection from the nominal (001) surface [the actual miscut from exact (001) being 1.28°], with the plane of incidence horizontal so that monochromator penetration by X-rays (albeit extinction-limited to a few µm) did not blur the fringe images. The monochromator-to-photoplate distance was 67 mm, sufficiently high to keep background scattering from the

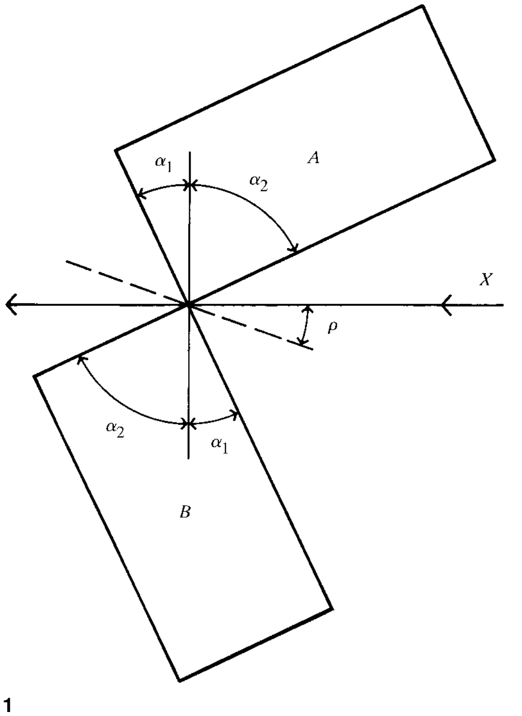

Figure 1
Vertical cross section through the biprism assembly. The two similar polished diamond bars A and B, cross sections 2 mm × 1 mm, meet along the biprism axis normal to the plane of the drawing. Ray X indicates the direction of X-rays transmitted by the biprism. For minimum deviation, the biprism assembly mirror line (dashed) coincides with direction X, and $\alpha_1 = \alpha_2 = 45°$. To obtain greater deviations the assembly is rotated about the biprism axis by angle ρ.

© 1999 International Union of Crystallography
Printed in Great Britain – all rights reserved

Table 1
Biprism interference observations: experimental parameters and fringe spacings.

Wavelength, λ (nm)	0.08	0.08	0.08	0.096	0.11
δ ($\times 10^{-6}$)	3.04	3.04	3.04	4.34	5.74
Biprism rotation, ρ (°)	15	20	24	20	0
Convergence angle, 2ε ($\times 10^{-6}$ rad)	14.0	15.8	18.1	22.7	23.0
Observation distance, P (m)	0.94	0.94	0.94	0.71	0.94
Linear overlap, O (μm)	13	15	17	16	21
Fringe spacing (calculated), F (μm)	5.70	5.04	4.41	4.22	4.79
Fringe spacing (observed), F (μm)	6.0	5.0	4.5	4.2	4.8

monochromator crystal less than ~10% of the intensity in the 004 reflection. This distance is included in the total distance P from biprism to photoplate, which determines the linear overlap O of the beams that issue from the biprism with angular convergence 2ε; $O = 2\varepsilon P$.

The expected interference fringe spacing F in the overlap region O, assuming illumination of the biprism from a distant source, is simply $F = \lambda/2\varepsilon$, independent of the observation distance P. Since $\varepsilon \propto \lambda^2$, F is proportional to $1/\lambda$, and the number of fringes within the overlap O, *i.e.* O/F, should be proportional to $P\lambda^3$. However, for fringes to form, O must not exceed D_t. In the apparatus set up at the SRS, three parameters could be varied; λ, ρ and P. To provide the best chance of success in the few days of beam time during which biprism experiments were conducted, these parameters were constrained to meet the following conditions: (i) the predicted F should be significantly greater than the 'geometrical' image resolution width sP/L, which is ~2.5 μm when $P = 0.9$ m; and (ii) P should be high enough to enable O to include at least the maxima of fringe orders −1, 0 and +1, but not so high as to extend O outside D_t.

Table 1 includes the parameter combinations that produced well measurable fringe patterns. For diamond, $\delta = 4.74\lambda^2 \times 10^{-4}$ with λ expressed in nm. When λ = 0.08 nm, only orders ±1 appeared in addition to the zero order. Hence F was derived from two fringe periods only. It was measured by video microscopy, averaging along segments of the fringe patterns. The measurement precision was about ±5%. In the fringe patterns obtained at longer wavelengths, exhibited in Figs. 2(*a*) and 2(*b*), four fringe periods were measurable, but orders ±2 were weak relative to orders ±1 and 0. (To display all orders with sufficient visibility on a single photographic print required holding back the exposure of the central orders when producing these prints.) In the short fringe segments shown at high magnification in Fig. 2, the combination of photon shot noise and emulsion grain clumps arising from short-range photoelectron tracks gives rise to a noisy picture. Noise effects are reduced by obliquely viewing the prints parallel to the fringes at a low grazing angle. Measurements of F were made on low-contrast high-magnification (×1400) prints of fringe pattern segments in the case of λ = 0.096 nm, and on similar prints and also on ×500 micrograph negatives in the case of λ = 0.11 nm, all with consistent findings, and estimated uncertainty within about ±3%.

One immediately realizable application of the above-described arrangement of biprism followed by monochromator is for independently measuring at selected wavelengths both the geometric size and the coherence properties of any X-ray source, whether actual or of virtual nature after beam conditioning by X-ray mirrors *etc.* For such measurements the non-dependence of biprism F on P can be exploited. Firstly, geometric size alone can be measured from the fringe visibility decay as fringe spacing F is reduced, provided the requirement that beam overlap $O \leq D_t$ is maintained. The reduction in F can be made by increasing ε *via* increase in ρ, while keeping $2\varepsilon P$ sufficiently low (preferably unchanged) by a proportionate reduction of P. For coherence measurement, a shortfall of D_t below that expected can be measured from fringe visibility decay as O is increased. The increase of O can be effected simply by increasing P while keeping F constant and as large as possible. One current method of estimating D_t is from contrast in the Fresnel fringe pattern accompanying radiographic images of objects such as fine fibres (Cloetens *et al.*, 1996). However, it is arguable that measuring D_t from the visibility decay in a *set* of fringes having invariant spacing should be a more objective and less noise-sensitive procedure. These advantages of the proposed biprism interference fringe

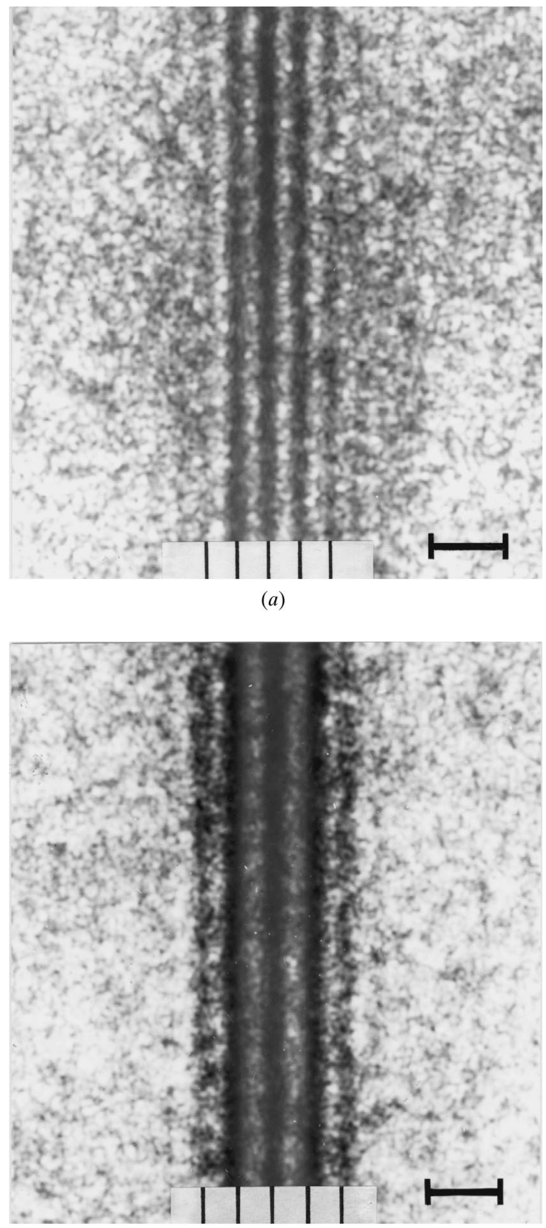

(*a*)

(*b*)

Figure 2
Biprism interference fringe patterns recorded on Ilford L4 nuclear plates, emulsion thickness 25 μm. Scale marks 10 μm. Calculated fringe positions shown. (*a*) Wavelength λ = 0.096 nm, rotation ρ = 20°, calculated fringe spacing F = 4.22 μm. (*b*) λ = 0.11 nm, ρ = 0°, calculated F = 4.79 μm.

method are shared with the phase grating self-imaging method using the Talbot effect (Erko *et al.*, 1996; Cloetens, Guigay *et al.*, 1997; Espeso *et al.*, 1998), but the biprism method is simpler.

Finally, it is worth remarking that diamond, though eminently suitable, is not essential for constructing the biprism assembly. For example, if polished sapphire bars were used the deviation reduction by the factor δ(sapphire)/δ(diamond) $\simeq$ 2/3 could generally be nullified by working with higher rotations ρ.

We thank the Director and Staff, Synchrotron Radiation Department, CCLRC Daresbury Laboratory, for provision of experimental facilities.

References

Born, M. & Wolf, E. (1980). *Principles of Optics*, 6th ed. Oxford: Pergamon Press.

Cloetens, P., Barrett, R., Baruchel, J., Guigay, J.-P. & Schlenker, M. (1996). *J. Phys. D*, **29**, 133–146.

Cloetens, P., Guigay, J. P., De Martino, C., Baruchel, J. & Schlenker, M. (1997). *Opt. Lett.* **22**, 1059–1061.

Cloetens, P., Pateyron-Salomé, M., Buffière, J. Y., Peix, G., Baruchel, J., Peyrin, F. & Schlenker, M. (1997). *J. Appl. Phys.* **81**, 5878–5885.

Erko, A. I., Aristov, V. V. & Vidal, B. (1996). *Diffraction X-ray Optics*, ch. 3. Bristol and Philadelphia: IOP Publishing.

Espeso, J. I., Cloetens, P., Baruchel, J., Härtwig, J., Mairs, T., Biasci, J. C., Marot, G., Salomé-Pateyron, M. & Schlenker, M. (1998). *J. Synchrotron Rad.* **5**, 1243–1249.

Lang, A. R. & Makepeace, A. P. W. (1999). *J. Phys. D*. In the press.

Lang, A. R., Makepeace, A. P. W., Martineau, P. M. & Cooper, M. A. (1997). *Diamond Relat. Mater.* **6**, 1226–1230.

Raven, C., Snigirev, A., Snigireva, I., Spanne, P., Souvorov, A. & Kohn, V. (1996). *Appl. Phys. Lett.* **69**, 1826–1828.

Snigirev, A., Kohn, V., Snigireva, I., Souvorov, A. & Lengeler, B. (1998). *Appl. Opt.* **37**, 653–662.